Spatiotemporal pattern formation in fractional reaction-diffusion systems with indices of different order

V. V. Gafiychuk[1,2] and B. Y. Datsko[2]
[1]*Physics Department, New York City College of Technology, CUNY, 300 Jay Street, Brooklyn, New York 11201, USA*
[2]*Institute for Applied Problems in Mechanics and Mathematics, National Academy of Sciences of Ukraine, Naukova Street 3b, Lviv 79053, Ukraine*
(Received 2 March 2008; published 16 June 2008)

The fractional reaction-diffusion system is investigated. The linear stage of the stability is studied for a two-component system with a different order of fractional derivatives for activator and inhibitor. Three different cases are considered: the derivative order for an activator is greater than that for an inhibitor, the inhibitor order derivative is greater than the activator one, and the orders of time derivatives are comparable. Based on the stability analysis, computer simulation of a Bonhoeffer–van der Pol type reaction-diffusion system with fractional time derivatives is performed, and the diversity of the pattern formation phenomena is shown.

DOI: 10.1103/PhysRevE.77.066210 PACS number(s): 82.40.Bj, 82.39.Rt, 82.40.Ck, 05.60.Cd

I. INTRODUCTION

Studying reaction-diffusion systems (RDSs), which have been prevalent for many years [1–3], is very important for understanding nonlinear phenomena in systems with fractional derivatives, which seems to be beneficial for describing complex heterogeneous systems where conventional approaches have failed [4,5]. The introduction of time or space derivatives of fractional order to a standard reaction-diffusion system, on one side, explains many anomalous properties, and on the other side, predicts new nonlinear phenomena that we could not have in conventional transport equations with local sources [6–12].

For complex heterogeneous systems, it is often difficult to perform a strict derivation of governing equations, and as a result, these models are often based on purely qualitative features. In this way, many well-known models, such as the Oregonator, Brusselator, Gierer-Meinhardt, and Gray-Scott models [1–3], were written phenomenologically to explain specific properties in complex systems and revolutionized our understanding of pattern-formation phenomena. Recent investigations, for example, show that morphogen formation in an inhomogeneous cell environment is better described by an anomalous diffusion model [15]. As a result, such models in real living systems are probably better described by fractional equations. In this case, the most important question is, what kind of solutions do these models possess?

Among the applications of time fractional differential equations, one can find the description of transport of fission cells during a tumor growth [16], as well as transport of a substance across a thin membrane [17]. Heterogeneous porous systems are often described by an effective medium of reaction-diffusion types with fractional derivatives [18]. A charge-carrier transport in disordered semiconductors due to non-Gaussian processes and multiple trapping can be much better described by fractional derivatives [19].

It should be noted that at present, reliable experimental media for investigating phenomena in reaction-diffusion systems with derivatives of fractional order can be created synthetically, with the help of circuits and modern solid-state technology [20–22]. In this case, we can design the layered solid-state distributive media, the corresponding layers of which have to be endowed with the properties inherent to the fractional order controllers [23,24]. As a result, each layer can be described by fractional differential equations and can even have its own fractional index.

II. MATHEMATICAL MODEL

The starting point of our consideration is the coupled reaction-diffusion equations with indices of different order [6–12],

$$\tau_1 \frac{\partial^{\alpha_1} n_1(x,t)}{\partial t^{\alpha_1}} = l_1^2 \frac{\partial^2 n_1(x,t)}{\partial x^2} + W(n_1,n_2,\mathcal{A}), \tag{1}$$

$$\tau_2 \frac{\partial^{\alpha_2} n_2(x,t)}{\partial t^{\alpha_2}} = l_2^2 \frac{\partial^2 n_2(x,t)}{\partial x^2} + Q(n_1,n_2,\mathcal{A}), \tag{2}$$

subject to Neumann,

$$\partial n_i/\partial x\big|_{x=0} = \partial n_i/\partial x\big|_{x=l_x} = 0, \quad i=1,2, \tag{3}$$

boundary conditions and with certain initial conditions. Here $n_1(x,t), n_2(x,t)$ are activator and inhibitor variables, $0 \le x \le l_x$, $\tau_i = (\tilde{\tau}_i)^{\alpha_i}$, $\tilde{\tau}_i, l_i$ are the characteristic times and lengths of the system, correspondingly, and $\mathcal{A}$ is an external parameter.

Time derivatives $\frac{\partial^{\alpha_i} n_i(x,t)}{\partial t^{\alpha_i}}$ on the left-hand side of Eqs. (1) and (2) instead of standard ones are the Caputo fractional derivatives in time of the order $0 < \alpha < 2$ and are represented as [25,26]

$$\frac{\partial^{\alpha}}{\partial t^{\alpha}} n_i(t) := \frac{1}{\Gamma(m-\alpha)} \int_0^t \frac{n_i^{(m)}(\tau)}{(t-\tau)^{\alpha+1-m}} d\tau,$$

where $m-1 < \alpha < m$, $m=1,2$. It should be noted that Eqs. (1) and (2) at $\alpha=1$ correspond to a standard reaction-diffusion system.

III. LINEAR STABILITY ANALYSIS

A. Spectrum analysis for $\alpha_1 = \alpha_2 = 1$

We consider RDSs with two variables: one of them is a variable with positive feedback and the second one is a vari-

able with a negative one. Specifically, these systems possess a variety of nonlinear phenomena investigated in recent decades [1–3]. Positive and negative feedbacks require a special form of nonlinearities. For example, the first source term which corresponds to the activator variable equation must be nonmonotonous and the second one can be monotonous. For our consideration, it is good to analyze nullclines of the system (1) and (2),

$$W(n_1,n_2,\mathcal{A})=0, \quad Q(n_1,n_2,\mathcal{A})=0. \tag{4}$$

Simultaneous solution of the system (4) leads to homogeneous distribution of $\bar{n}_1$ and $\bar{n}_2$. Such analysis is very well known at $\alpha_1=\alpha_2=1$, and the stability of the steady-state solutions of the system (1) and (2) corresponding to a homogeneous equilibrium state is determined by the eigenvalue problem

$$\lambda\,\delta\mathbf{n}=F(k)\,\delta\mathbf{n}, \tag{5}$$

where $\lambda_{1,2}=\frac{1}{2}(\mathrm{tr}\,F\pm\sqrt{\mathrm{tr}^2\,F-4\,\det F})$ are eigenvalues of the matrix

$$F(k)=\begin{pmatrix} a_{11}(k)/\tau_1 & a_{12}/\tau_1 \\ a_{21}/\tau_2 & a_{22}(k)/\tau_2 \end{pmatrix},$$

$k=\frac{\pi}{l_s}j$, $j=1,2,\ldots$, $a_{11}(k)=a_{11}-k^2l_1^2$, $a_{11}=W'_{n_1}$, $a_{12}=W'_{n_2}$, $a_{21}=Q'_{n_1}$, $a_{22}(k)=a_{22}-k^2l_2^2$, $a_{22}=Q'_{n_2}$ (all derivatives are taken at homogeneous equilibrium states $W=Q=0$), and $\delta\mathbf{n}=(\Delta n_1,\Delta n_2)^T$ are new variables $\Delta n_i=n_i-\bar{n}_i$.

For $\alpha_1=\alpha_2=1$ and $k=0$ at the conditions

$$\mathrm{tr}\,F(0)>0, \quad \det F(0)>0, \tag{6}$$

we can have a Hopf bifurcation. For $k\neq 0$, it is possible that at a certain value of k_0 eigenvalues $\lambda_{1,2}$ are real and one of them is greater than zero (a Turing bifurcation). The conditions of this instability are

$$\mathrm{tr}\,F<0, \quad \det F(0)>0, \quad \det F(k_0)<0. \tag{7}$$

We can rewrite inequality (6) as $a_{11}>-a_{22}\tau_1/\tau_2$ according to time frequency oscillation $\omega=\sqrt{\det F(0)/(\tau_1\tau_2)}$ and inequality (7) as [1–3]

$$a_{11}>-a_{22}(l_1^2/l_2^2)+2\sqrt{\det F(0)}(l_1/l_2) \tag{8}$$

according to wave numbers

$$k_0=\sqrt[4]{\det F(0)}/\sqrt{l_1l_2}. \tag{9}$$

Instability conditions for these two types of bifurcations are realized due to positive feedback ($a_{11}>0$), and at $\tau_1/\tau_2\to 0$ and $l_1/l_2\to 0$ they coincide and approach the extremum point (or points) of $W(n_1,n_2,\mathcal{A})=0$.

B. Fractional RDS when $\alpha_1=\alpha_2$

Local dynamics. It was shown that in the case of fractional derivative index $\alpha_1=\alpha_2=\alpha$ ($0<\alpha<2$), the system (1) and (2) is unstable at [11,12,27]

$$|\arg(\lambda_i)|<\alpha\pi/2. \tag{10}$$

This condition can be easily transformed to an explicit form. In fact, the system in a linear approach can be presented as $\frac{\partial^\alpha\delta\mathbf{n}}{\partial t^\alpha}=F\,\delta\mathbf{n}$, where $\delta\mathbf{n}$ is the perturbation vector. The marginal value $\alpha=\alpha_0=\frac{2}{\pi}|\arg(\lambda_i)|$, which changes the stability state, follows from the conditions (10) and is given by the formula [11,12]

$$\alpha_0=\frac{\pi}{2}\tan^{-1}\left|\frac{\mathrm{Im}\,\lambda}{\mathrm{Re}\,\lambda}\right|_{\mathrm{Re}\,\lambda>0}\cup 2-\frac{\pi}{2}\tan^{-1}\left|\frac{\mathrm{Im}\,\lambda}{\mathrm{Re}\,\lambda}\right|_{\mathrm{Re}\,\lambda<0}. \tag{11}$$

It should be noted that in the case of the fractional derivative index, the Hopf bifurcation is not connected with the condition $a_{11}>0$ and can hold even if $a_{11}<0$ when the fractional derivative index is sufficiently large [12].

Fractional RDS. Linear stability analysis shows that the conditions of the Turing bifurcation are the same as for the standard system. Having a critical value of α for homogeneous perturbation $k=0$ (11), we can analyze if there is a condition in which the Hopf bifurcation for $k=0$ is not realized but at the same time conditions of the Hopf bifurcation for $k\neq 0$ become true. In particular, this situation is considered in [11,12],

$$\mathrm{tr}\,F(0)<0, \quad 4\,\det F(0)<\mathrm{tr}^2F(0),$$

$$4\,\det F(k_0)>\mathrm{tr}^2\,F(k_0). \tag{12}$$

In this case, the instability conditions are

$$\alpha>\alpha_0(k_0)=2-\frac{\pi}{2}\tan^{-1}\left(4\frac{\det F(k_0)}{\mathrm{tr}^2F(k_0)}-1\right)^{1/2}. \tag{13}$$

The simplest way to satisfy the last condition is to estimate the optimal value of $k=k_0$,

$$k_0=2\left(\frac{-a_{12}a_{21}}{l_1^2/\tau_2-l_2^2/\tau_1}\right)^{1/2}. \tag{14}$$

Having obtained Eq. (14), we can estimate the marginal value of α_0 [11], where

$$\left|\frac{\mathrm{Im}\,\lambda}{\mathrm{Re}\,\lambda}\right|_{\mathrm{Re}\,\lambda<0}=\frac{(-4a_{12}a_{21}\tau_1\tau_2)^{1/2}}{\left|(a_{11}\tau_2-a_{22}\tau_1)\frac{l_1^2\tau_2+l_2^2\tau_1}{l_1^2\tau_2-l_2^2\tau_1}\right|-a_{11}\tau_2-a_{22}\tau_1}.$$

Since the conditions of the Turing bifurcation for the case $\alpha\neq 1$ are determined by the formulas (8) and (9) in the nonlinear dynamics, nonhomogeneous structures can be stable or oscillatory [10,11] depending on the value of fractional derivative index α.

C. Fractional RDS when $\alpha_1=2\alpha_2$

Let us consider the case in which $\alpha_1=2\alpha_2=2\alpha$ ($0<\alpha<1$). Due to properties of the Caputo derivatives [24] by simple substitution, we obtain the system of three equations

$$\frac{\partial^\alpha n_1(x,t)}{\partial t^\alpha}=\frac{n_3}{\tau_1^{1/2}}, \tag{15}$$

$$\tau_2\frac{\partial^\alpha n_2(x,t)}{\partial t^\alpha}=l_2^2\frac{\partial^2 n_2(x,t)}{\partial x^2}+Q(n_1,n_2,\mathcal{A}), \tag{16}$$

$$\tau_1^{1/2}\frac{\partial^\alpha n_3(x,t)}{\partial t^\alpha} = l_1^2\frac{\partial^2 n_1(x,t)}{\partial x^2} + W(n_1,n_2,\mathcal{A}). \quad (17)$$

Stability analysis of the system (15)–(17) can be made by substituting solutions in the form $\delta n_i \sim \cos(kx)$ and considering a system of three linear differential equations, the Jacobian of which is

$$J = \begin{pmatrix} 0 & 0 & 1/\tau_1^{1/2} \\ a_{21}/\tau_2 & a_{22}(k)/\tau_2 & 0 \\ a_{11}(k)/\tau_1^{1/2} & a_{12}/\tau_1^{1/2} & 0 \end{pmatrix}. \quad (18)$$

In this case, the characteristic equation has the form

$$\lambda^3 + \lambda^2 b + \lambda c + d = 0, \quad (19)$$

where

$$b = -a_{22}(k)/\tau_2, \quad c = -a_{11}(k)/\tau_1, \quad d = \det F(k). \quad (20)$$

Here we would like to single out several characteristic limits, which can be analyzed analytically in order to understand what kind of effects we meet here.

Limit $0 < \det F(k) \ll 1$. Let us first consider a small value of $\det F(k)$. Then, by using the perturbation technique, we can find the roots, which are determined by the following expressions:

$$\lambda_1 \approx \det F(k)/[a_{11}(k)\tau_2],$$

$$\lambda_{2,3} \approx \frac{1}{2}\left(\frac{a_{22}(k)}{\tau_2} \pm \sqrt{\frac{a_{22}^2(k)}{\tau_2^2} + \frac{4a_{11}(k)}{\tau_1}}\right). \quad (21)$$

In the case of local dynamics ($k=0$) at $a_{11}>0$ and sufficiently small $\det F(0)$, all roots lie on the real axis [28]. The first root λ_1 can change sign depending on the sign of $\det F(0)$. When nullclines are practically tangent to each other at $\det F \approx 0$, the system is unstable, practically for all values of α. It should be noted that the condition $\det F(0) > 0$ can be rewritten as $dn_2/dn_1|_{Q=0} > dn_2/dn_1|_{W=0}$, which means that the second nullcline ($Q=0$) has a greater slope than the first one ($W=0$). This is why a positive value of the determinant $\det F(0)$ does not lead to instability. The second root λ_2 is positive because the value of the radical is greater than $|a_{22}|$ ($a_{11}>0$ inside the interval where the positive feedback is realized). Consequently, only the third root λ_3 is always negative.

If $k \neq 0$ for a certain value of k_0, the value of $\det F(k_0)$ becomes less than zero and the first eigenvalue can be positive if $a_{11}(k)>0$. Moreover, coefficient $a_{22}(k)$ is negative even if the coefficient $a_{11}(k)$ is negative for large values of k and, consequently, homogeneous oscillations will depress the emergence of inhomogeneous dissipative structures with $k \gg l_1^{-1}$ at $|\det F(0)| \ll 1$. But for $k \sim k_0$ defined from Eq. (9), it appears that the conditions of the Turing instability in nonlinear dynamics will come into play with conditions of homogeneous oscillations, and we expect a complicated pattern formation.

General case $\alpha_1 = 2\alpha_2 = 2\alpha$ $(0 < \alpha < 1)$. In this case by simple substitution $\lambda = u - b/3$, and introducing the new parameters

$$p = c - b^2/3, \quad q = d - bc/3 + 2b^3/27, \quad (22)$$

we can obtain the depressive cubic equation $u^3 + pu + q = 0$ and eignevalues of the equation (19) are represented by Cardano formulas,

$$\lambda_1 = A + B - b/3, \quad (23)$$

$$\lambda_2 = -(A+B)/2 + i\sqrt{3}(A-B)/2 - b/3, \quad (24)$$

$$\lambda_3 = -(A+B)/2 - i\sqrt{3}(A-B)/2 - b/3, \quad (25)$$

where $A = \sqrt[3]{-q/2 + \sqrt{\Delta}}$, $B = \sqrt[3]{-q/2 - \sqrt{\Delta}}$, $\Delta = (q/2)^2 + (p/3)^3$.

Let us analyze eigenvalues of the equation (19). If the value of $\Delta < 0$, then all roots of Eq. (19) are real. In this case, if at least one of the roots is positive, then the system will be unstable and will lead to oscillations for practically any value of α. We can see that at $A+B > b/3$, the first root leads to instability and the second two could be less than zero. In the opposite situation, the first one is negative and one root of the two others leads to instability. So, as a result, the system could always be unstable either to the first eigenvalue or to one of the second two. A detailed analysis of the eigenvalues for specific nonlinearities is given in the next section. Here, we would like to conclude with just the general properties of the system.

If $\Delta > 0$, then A,B and consequently λ_1 are real and the roots λ_2,λ_3 are complex. In this case if $A+B > b/3$, then the system is unstable according to any value of α. At $A+B < b/3$, the first root is real and negative and the system could be unstable for a certain value of α $(\alpha > \alpha_0)$,

$$\alpha_0(k) = \frac{2}{\pi}\tan^{-1}\left|\frac{\sqrt{3}[A(k) - B(k)]}{2b(k)/3 + A(k) + B(k)}\right|. \quad (26)$$

As a result of this instability, we can expect nonlinear oscillations that could be homogeneous for $k=0$ if $\alpha_0(0) < \alpha_0(k)$ and nonhomogeneous $(k \neq 0)$ if $\alpha_0(k) < \alpha_0(0)$.

It should be noted that for $k \neq 0$, conditions of instability according to this wave number are stricter than homogeneous oscillations. This means that homogeneous oscillations arise at smaller values of α_0 than inhomogeneous ones. So, the conditions of Turing instability (8) do not depend on α_0 and can be easily realized in the system; we can expect complicated dynamics of pattern formation when simultaneous conditions of instability become true.

D. Fractional RDS when $2\alpha_1 = \alpha_2$

In the case $2\alpha_1 = \alpha_2 = 2\alpha$ $(0 < \alpha < 1)$, the characteristic equation

$$\det(J - \lambda I) = \begin{pmatrix} a_{11}(k)/\tau_1 - \lambda & a_{12}/\tau_1 & 0 \\ 0 & -\lambda & 1/\tau_2^{1/2} \\ a_{21}/\tau_2^{1/2} & a_{22}(k)/\tau_2^{1/2} & -\lambda \end{pmatrix} = 0 \quad (27)$$

is represented by Eqs. (23)–(25), where coefficients b and c interchange their values,

$$b = -a_{11}(k)/\tau_1, \quad c = -a_{22}(k)/\tau_2. \tag{28}$$

The similar speculation as before shows that the system could be unstable practically for all values of α. In this case for the roots (19), we have one negative root and two complex roots, the real part of which is greater than zero.

At the limit $0 < \det F(k) \ll 1$, the three roots are real and two of them ($\lambda_{2,3}$) are positive,

$$\lambda_1 \approx \det F(k)/[a_{22}(k)\tau_1],$$

$$\lambda_{2,3} \approx \frac{1}{2}\left(\frac{a_{11}(k)}{\tau_1} \pm \sqrt{\frac{a_{11}^2(k)}{\tau_1^2} + \frac{4a_{22}(k)}{\tau_2}}\right). \tag{29}$$

In fact, considering local dynamics and recalling that the first variable is an activator $[a_{11}(0) > 0]$ and the second one is an inhibitor $[a_{22}(0) < 0]$, we conclude that the first root is negative $[\det F(0) > 0]$ and the second and third eigenvalues $\lambda_{2,3}$ are greater than zero. If the expression inside the radical is positive in Eq. (29),

$$a_{11}^2 + 4a_{22}\tau_1^2/\tau_2 > 0, \tag{30}$$

we have two real eigenvalues greater than zero. As a result, instability can have a place for sufficiently small values of α_1, α_2. At $a_{11}^2 + 4a_{22}\tau_1^2/\tau_2 < 0$, we have the minimum value of α_0 ($\alpha > \alpha_0$),

$$\alpha_0 = \sqrt{\left|1 + \frac{4a_{22}\tau_1^2}{a_{11}^2\tau_2}\right|},$$

when oscillations start to arise. It is easy to obtain that $\alpha_0(k) > \alpha_0$ and, as a result, the conditions of the Hopf bifurcation for $k=0$ are realized earlier. In this case, conditions of the Turing bifurcation (8) and (11) are valid and we can obtain the interaction of these two instabilities and complex pattern formation.

E. Fractional RDS with arbitrary rational α_1, α_2

With arbitrary rational α_1 and α_2 (for example, $\alpha_1 > \alpha_2$), by a certain substitution, the system can be transformed to the set of many differential equations. In fact, the fractional derivative index being the "greatest common factor" α of the values $\alpha_1 = m\alpha$ and $\alpha_2 = p\alpha$ simultaneously, $m, p \in \mathbb{N}$, we obtain the system of $m+p$ differential equations. In this case, the matrix characteristic equation

$$\det(J - \lambda I) = \begin{vmatrix}
-\lambda & 0 & \tau_1^{-1/m} & 0 & \cdots & 0 & 0 & 0 & \cdots & 0 \\
0 & -\lambda & 0 & 0 & \cdots & 0 & 0 & \tau_1^{-1/m} & \cdots & 0 \\
0 & 0 & -\lambda & \tau_1^{-1/m} & \cdots & \cdots & 0 & 0 & \cdots & 0 \\
\cdots & \cdots & \cdots & -\lambda & \cdots & \tau_1^{-1/m} & \cdots & \cdots & \cdots & \cdots \\
\cdots & \cdots & \cdots & \cdots & \cdots & \cdots & \cdots & \cdots & \cdots & \cdots \\
0 & 0 & 0 & 0 & \cdots & -\lambda & \tau_1^{-1/m} & 0 & 0 & 0 \\
a_{11}(k)/\tau_1^{(1/m)} & a_{12}/\tau_1^{(1/m)} & 0 & 0 & \cdots & 0 & -\lambda & 0 & \cdots & 0 \\
\cdots & \cdots & \cdots & \cdots & \cdots & \cdots & \cdots & \cdots & \cdots & \cdots \\
0 & 0 & 0 & 0 & \cdots & 0 & \cdots & -\lambda & \tau_2^{-1/p} & 0 \\
0 & 0 & 0 & 0 & \cdots & 0 & \cdots & 0 & -\lambda & \tau_2^{-1/p} \\
a_{21}/\tau_2^{(1/p)} & a_{22}(k)/\tau_2^{(1/p)} & 0 & 0 & \cdots & 0 & \cdots & 0 & \cdots & -\lambda
\end{vmatrix} = 0$$

can be transformed to the polynomial characteristic equation of the form

$$(-\lambda)^{m+p} + (-1)^{p-1}\frac{a_{22}(k)}{\tau_2}(-\lambda)^m + (-1)^{m+1}\frac{a_{11}(k)}{\tau_1}(-\lambda)^p + (-1)^{m+p}\det F = 0. \tag{31}$$

The solution of such an equation can be obtained numerically. At the small value of $\epsilon = \det F$, it is always possible to find the roots with the value close to zero,

$$\lambda_i \approx (\tau_2\epsilon/a_{22})^{1/m} \quad \text{if } \alpha_1 < \alpha_2, \quad i \in \overline{1,m}, \tag{32}$$

$$\lambda_i \approx (\tau_1\epsilon/a_{11})^{1/p} \quad \text{if } \alpha_1 > \alpha_2, \quad i \in \overline{1,p} \tag{33}$$

and to determine where they are greater than zero entailing the instability. Of course, the system can be unstable owing to the other eigenvalues λ_j, as it was in the situation considered above. Having found these eigenvalues, we can establish the conditions sufficient for instability.

Here we explore numerically the system dynamics when the parameters of the derivative indices are different and change from small values practically to two. To be specific, we employ a two-component reaction-diffusion system (1) and (2) for the source terms determined by a Bonhoeffer–van der Pol kinetics. Such an approach is very popular for a

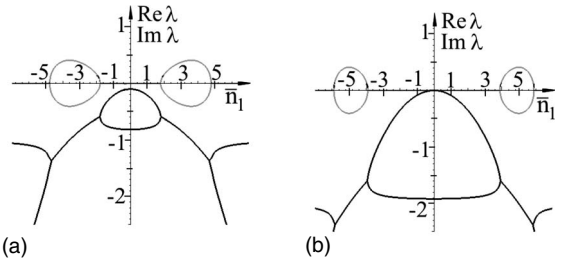

FIG. 1. Imaginary (gray lines) and real parts (black lines) of eigenvalues as a function of $\bar{n}_1$ at $\alpha_1=\alpha_2$ for $k=0$ (a) and $k=1$ (b). The other parameters are $\beta=2$, $\tau_1=12$, $\tau_2=1$, $l_1^2=0.1$, $l_2^2=1$.

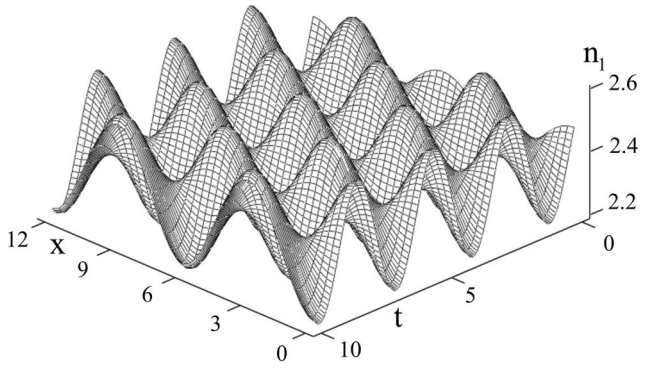

FIG. 2. The oscillatory structures obtained from numerical simulations of the system (1),(2). Dynamics of variable n_1 on the time interval (0,10) for $\alpha_1=1.9$, $\alpha_2=1.75$, $\tau_1=1$, $\tau_2=1$, $l_1^2=0.1$, $l_2^2=1.0$, $\mathcal{A}=-10$, $\beta=3$. Initial conditions are $n_1^0=\bar{n}_1-0.05\cos(k_0x)$, $n_2^0=\bar{n}_2-0.05\cos(k_0x)$.

standard reaction-diffusion system, and a lot of recent publications are devoted to finding nonlinear solutions in such media (see, for example, [29–31]).

IV. SOLUTIONS OF THE COUPLED FRACTIONAL RDS FOR A BONHOEFFER–VAN DER POL TYPE RDS

As an example, we consider here a Bonhoeffer–van der Pol type RDS with cubical nonlinearity (see Refs. [2,3,11,12]). In this case, the source term for an activator variable is nonlinear, $W=n_1-n_1^3-n_2$, and it is linear for the inhibitor one, $Q=-n_2+\beta n_1+\mathcal{A}$. The homogeneous solution of variables $\bar{n}_1$ and $\bar{n}_2$ can be determined from the system of equations $W=Q=0$, and for determination of $\bar{n}_1$ we have the cubic algebraic equation

$$(\beta-1)\bar{n}_1+\bar{n}_1^3/3+\mathcal{A}=0. \tag{34}$$

Calculation of the coefficients a_{ij}: $a_{11}=(1-\bar{n}_1^2)$, $a_{12}=-1$, $a_{21}=\beta$, $a_{22}=-1$ at homogeneous state (34) makes it possible to investigate the eigenvalues of the system explicitly. As a result, we can see that at $\tau_1/\tau_2\to 0$ and $l_1/l_2\to 0$ in a standard RDS, the instability domain is determined at $|\bar{n}_1|<1$. In this case, the simultaneous conditions of the Hopf (6) and the Turing (7) bifurcations are realized.

The case $\alpha_1=\alpha_2>1$. Real and imaginary parts of the eigenvalues for $k=0$ obtained numerically for each particular point $\bar{n}_1$ as a solution of the equation for a certain relationship between τ_1 and τ_2 are presented in Fig. 1(a). For these parameters, we see that the real part of the roots is always less than zero and the imaginary one on some interval of $\bar{n}_1$ becomes nonzero. In this case, when the fractional derivative index becomes greater than some critical value $\alpha_0=\frac{\pi}{2}\tan^{-1}(\mathrm{Im}\,\lambda/\mathrm{Re}\,\lambda)$, the instability condition (11) holds true. So, at $\alpha>\alpha_0$ we have homogeneous oscillations. In this case, at the values of $\alpha_0>1.5$, instability conditions are taking place in the interval $1.8\lesssim|\bar{n}_1|\lesssim 4.5$.

A similar plot can be presented for the eigenvalues when wave number $k\neq 0$ (for example, $k=1$). In Fig. 1(b), imaginary parts of the eigenvalues are presented for the same parameters of the system. As we can see from this figure, when nullclines have an intersection point in the interval $|\bar{n}_1|$ between 4.5 and 6, the system is stable according to homogeneous oscillations. At a certain value of α, instability conditions are possible to realize for $k=1$. This means that at least perturbations with this wave number are unstable (they are unstable for oscillatory fluctuations). This situation is qualitatively different from the integer RDS, whether the Turing ($k\neq 0$) or Hopf ($k=0$) bifurcation takes place. This depends on which conditions are easier to realize. In the system under consideration, we can choose the parameter $4.5<\bar{n}_1<6$ when we do not have a standard Hopf or Turing bifurcation at all. Nevertheless, we obtained that the conditions for the Hopf bifurcation can be realized for nonhomogeneous perturbations with wave numbers $k\neq 0$ [11,12].

This phenomenon is inherent to the system with different order of fractional derivatives if the difference between them is not so substantial. In the case considered above, when one index is two times greater than the other, the conditions of the existing Hopf bifurcation for nonhomogeneous perturbations becomes stricter than the conditions of the standard Hopf bifurcation for $k=0$. When the indices are comparable, then the domain of existing oscillatory instability conditions is sufficiently wide.

The result of computer simulation of such nonlinear nonhomogeneous oscillations for $\alpha_1\gtrsim\alpha_2$ is presented in Fig. 2. For a numerical simulation of the system (1),(2), with corresponding initial and boundary conditions, we used the finite-difference schemes based on Grünwald-Letnikov and Riemann-Liouville definitions [13,24,25], the application of which is considered in detail in Ref. [14].

It should be noted that the presented phenomena are realized outside the increasing path of nullcline $W=0$ ($|\bar{n}_1|>1$) and these phenomena are typical for different relationships between system parameters.

The case $\alpha_1>\alpha_2$ $(0<\alpha_1,\alpha_2<2)$. The investigation of the eigenvalues for $k=0$, depending on parameter $\bar{n}_1$, is presented in Fig. 3(a). We see that one real root is always less than zero. The roots of two others at $|\bar{n}_1|>\bar{n}_1^0$ are complex-conjugate roots. At $|\bar{n}_1|<\bar{n}_1^0$, these roots become real and positive. As a result of these conditions, instability in the system takes place practically for all values of α.

Except for homogeneous oscillations, a condition of the Turing instability becomes true if the ratio of $l_1/l_2\ll 1$. As an example, the plot of the eigenvalues for $k=1$ is presented in Fig. 3(b), where at $|\bar{n}_1|<\bar{n}_1^k$ all of the roots are real and one of them corresponds to stationary inhomogeneous structures.

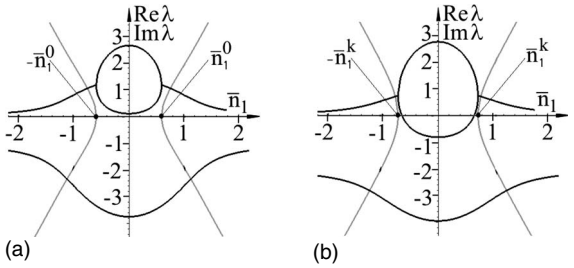

FIG. 3. Imaginary (gray lines) and real parts (black lines) of eigenvalues as a function of $\bar{n}_1$ obtained from solution of Eq. (19) at $\alpha_1=2\alpha_2$ for $k=0$ (a) and $k=1$ (b). The other parameters are $\beta=1.1$, $\tau_1=0.1$, $\tau_2=1$, $l_1^2=0.1$, $l_2^2=1$.

At $|\bar{n}_1|<\bar{n}_1^k$, we could have inhomogeneous oscillations of the structures if the conditions of this instability are softer than conditions of homogeneous oscillations. But this domain is very narrow in parameters, and practically for all parameters we have $\alpha_0<\alpha_0(k)$.

Computer simulation of the system is presented in Figs. 4 and 5. In Fig. 4(a), we can see the simplest pattern formation scenario corresponding to homogeneous oscillations when homogeneous solution $\bar{n}_1$ is close to zero. By moving beyond this point by increasing $\mathcal{A}$, homogeneous oscillations are slightly modulated by the inhomogeneous mode. At a certain value of $\mathcal{A}$, the Turing instability appears and we get very complicated patterns oscillating in space and time [Fig. 4(b)]. A successive increase of $\mathcal{A}$ to $\bar{n}_1=1$ again leads to slightly inhomogeneous oscillations and at a certain $\bar{n}_1>1$ the system becomes stable.

By increasing the fractional derivative index, we revealed spatiotemporal oscillations in the stability domain $|\bar{n}_1|>1$ for the Turing bifurcation [Figs. 4(c) and 4(d)]. The problem is that homogeneous oscillations are not connected with instability domain $|\bar{n}_1|<1$, because these oscillations are determined by condition (11). If they have a large amplitude and period, the variables n_1, n_2 fall into the region where conditions of the Turing instability become true ($|\bar{n}_1|<1$). As a result, space structures start to arise. If these oscillations are sufficiently slow compared to the characteristic time of the inhomogeneous structure formation, the developing structures become of greater amplitude. Due to the high value of α ($\alpha<2$), oscillations continue their path through the stable part of nullclines [($|\bar{n}_1|>1$)] and inhomogeneous structures start to destroy themselves. After that, a new period of structure formation begins to rise. Several plots of such spatiotemporal structures are presented in Figs. 4(c) and 4(d).

Computer simulation shows that the interplay between the Hopf and Turing bifurcations, which leads to complicated dynamics, is typical for a wide spectrum of parameters α from a small one such as $\alpha=0.1$ to 1. For example, typical spatiotemporal structures for different parameters of α are presented in Figs. 5(a)–5(c). These spatiotemporal patterns emerge as a result of the interplay between the Hopf and Turing bifurcations. In fact, according to Fig. 3, eigenvalues for $k=0$ and 1 in the system parameters are practically the same in the vicinity of the point $|\bar{n}_1|=0$. In this case, different initial conditions for $k\neq 0$ lead to more complicated spa-

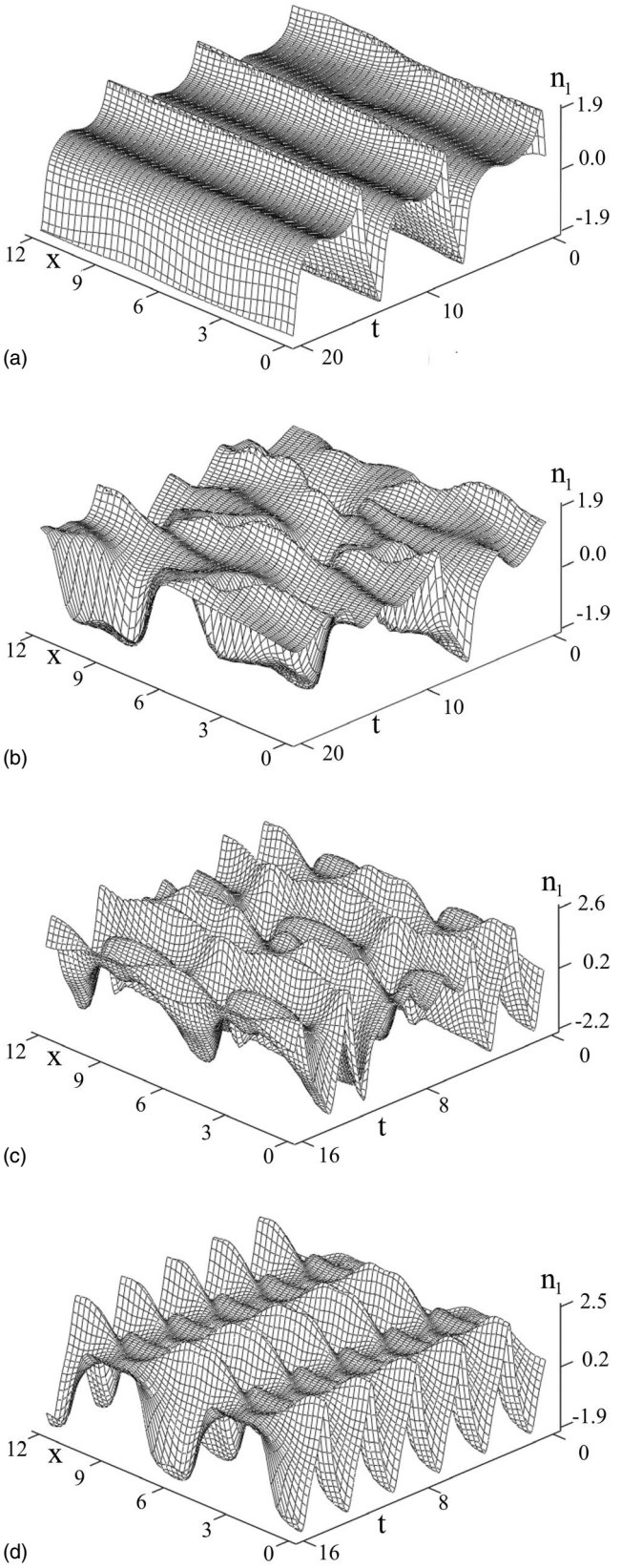

FIG. 4. Spatiotemporal structures obtained from computer simulation of the system (1),(2). Dynamics of variable n_1 for $\alpha_1=1.5$, $\alpha_2=0.75$, $\mathcal{A}=-0.2$ (a); $\alpha_1=1.5$, $\alpha_2=0.75$, $\mathcal{A}=-0.3$ (b); $\alpha_1=1.8$, $\alpha_2=0.9$, $\mathcal{A}=-0.5$ (c); $\alpha_1=1.8$, $\alpha_2=0.9$, $\mathcal{A}=-0.7$ (d). The other parameters are $\tau_1=0.1$, $\tau_2=1$, $l_1^2=0.1$, $l_2^2=1.0$, $\beta=1.1$.

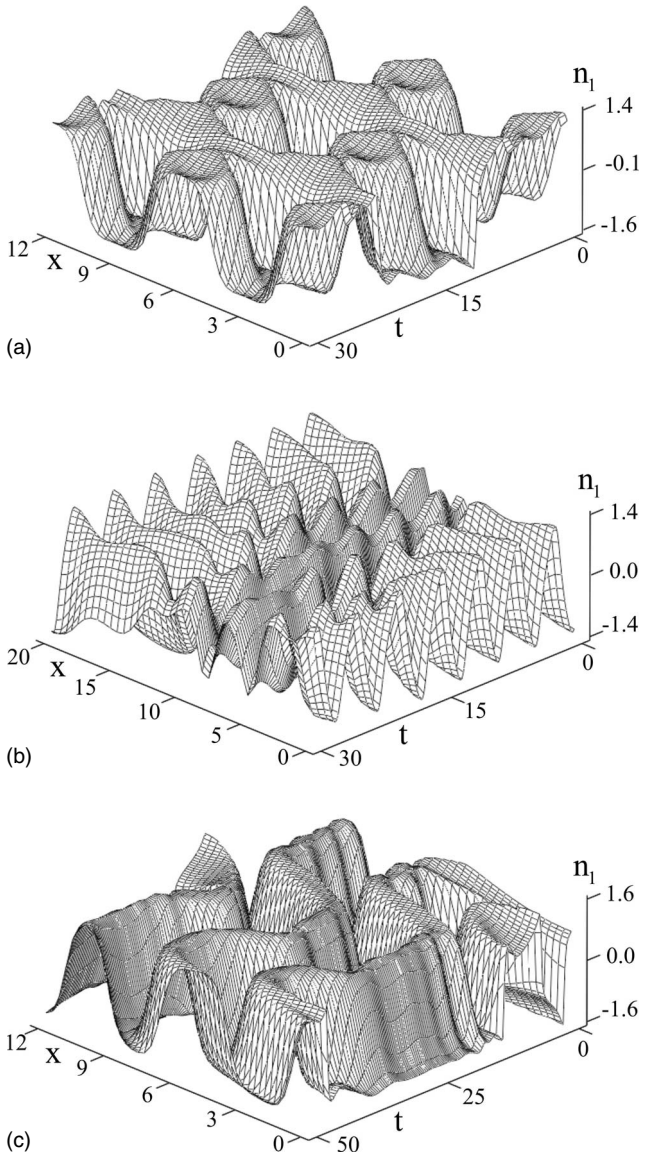

FIG. 5. Pattern formation scenario for $\alpha_1=1.0$, $\alpha_2=0.5$, $\mathcal{A}=-0.01$, $\beta=1.1$ (a); $\alpha_1=1.2$, $\alpha_2=0.6$, $\mathcal{A}=-0.1$, $\beta=2.0$ (b); $\alpha_1=0.9$, $\alpha_2=0.45$, $\mathcal{A}=-0.01$, $\beta=1.1$ (c). The other parameters are $\tau_1=0.1$, $\tau_2=1$, $l_1^2=0.1$, $l_2^2=1.0$.

tiotemporal patterns (see Fig. 5), similar to those displayed in Fig. 4. If the plot in Fig. 4 shows a practically uncorrelated scenario of patterns, the results presented by Figs. 5(a)–5(c) display complicated inhomogeneous structure oscillations for different values of α. The drawn profile of complex "zigzag" oscillations is given in Fig. 5(c). It should be noted that the form of these structures is strongly dependent on the fractional derivative indices as well as initial conditions and parameters of the system under consideration.

The obtained scenario of pattern formation is typical for the general case $\alpha_1>\alpha_2$. We can find that at certain parameters the solutions may have a simple form of homogeneous oscillations or stationary inhomogeneous structures as well, and can correspond to spatiotemporal structures similar to those presented in Figs. 4 and 5. In addition to homogeneous oscillation or stationary structure formation inherent to a

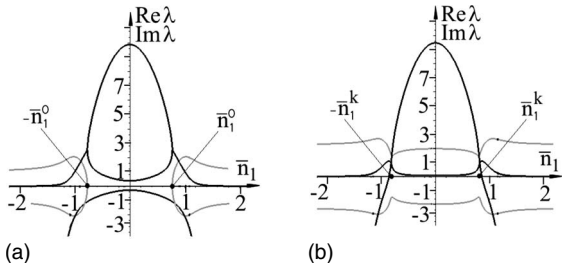

FIG. 6. Imaginary (gray lines) and real parts (black lines) of eigenvalues as a function of $\bar{n}_1$ at $2\alpha_1=\alpha_2$ for $k=0$ (a) and $k=1$ (b). The other parameters are $\beta=1.1$, $\tau_1=0.1$, $\tau_2=1$, $l_1^2=0.1$, $l_2^2=1$.

standard system with integer derivatives, the system considered here with indices $\alpha_1>\alpha_2$ possesses more complicated nonlinear dynamics. We can conclude that for $\alpha_1\gtrsim\alpha_2$, the possible solutions are even more diverse. In fact, if in the

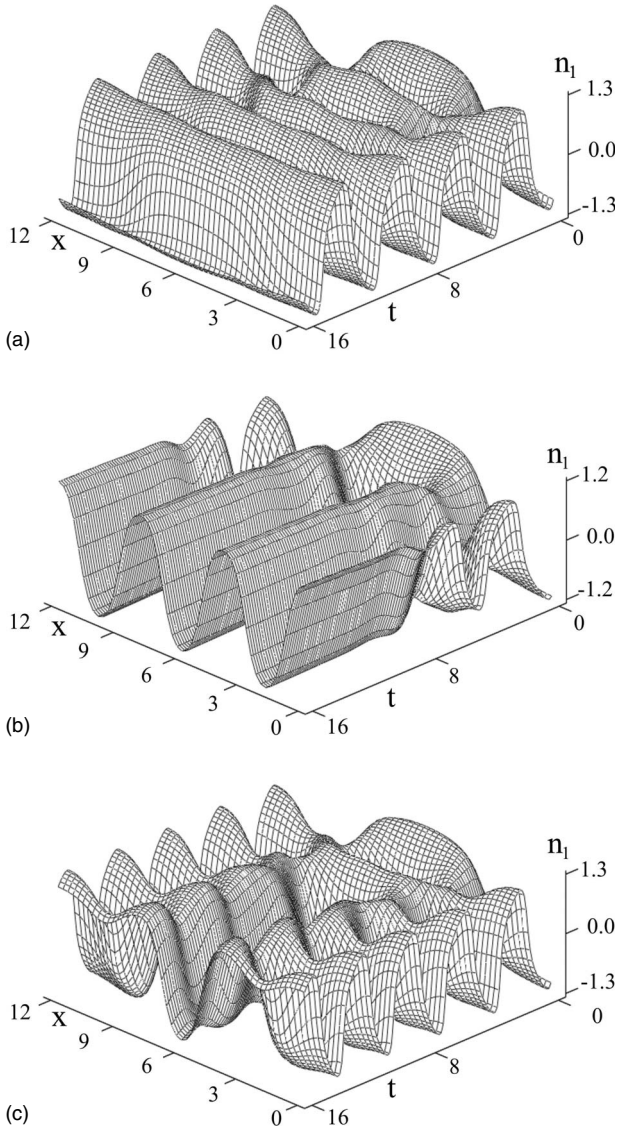

FIG. 7. Pattern formation scenario for $\alpha_1=0.55$, $\alpha_2=1.1$ (a); $\alpha_1=0.45$, $\alpha_2=0.9$ (b); $\alpha_1=0.5$, $\alpha_2=1.0$ (c). The other parameters are $\tau_1=0.4$, $\tau_2=1$, $l_1^2=0.1$, $l_2^2=1.0$, $A=-0.01$, $\beta=1.1$.

case $\alpha_1/\alpha_2=2$ we do not have a domain where oscillatory instability conditions for inhomogeneous wave numbers are realized, then at comparable values of $\alpha_1 \gtrsim \alpha_2$ it is easy to find a domain where $\alpha(k)<\alpha_0$. As a result, we have oscillatory inhomogeneous structure formation [11,12] (Fig. 2).

The case $\alpha_1<\alpha_2$ $(0<\alpha_1,\alpha_2<2)$. In the analysis of the case $\alpha_1<\alpha_2$, we start with $2\alpha_1=\alpha_2$. The dependence of eigenvalues as a function of $\bar{n}_1$ is presented in Fig. 6. Similar to the case considered above at $|\bar{n}_1|>\bar{n}_1^0$, two roots are complex and one is real. At certain parameters of n_1^0, all three roots become real, two of them are positive, and the system loses its stability at any value α. In the vicinity of $n_1 \approx 0, \beta \simeq 1$, the roots correspond to analytical solutions (21).

At the same time, at $l_1/l_2 \ll 1$ and $|\bar{n}_1|<1$ the system is unstable according to the Turing instability. The plot of the roots of characteristic equation (19) for $k=1$ is presented in Fig. 6(b). At $|\bar{n}_1|<\bar{n}_1^k$, the system has one positive real root of great value and two complex-conjugate roots. Namely, the first root is responsible for stationary pattern formation. By increasing α, we can always obtain homogeneous oscillations, which, on the one hand, will lead to oscillations of the structures, and on the other hand can destroy them and lead to homogeneous oscillations.

The typical scenario of the structure formation in the case $2\alpha_1=\alpha_2$ is not so diverse as for the case considered above, and at a wide limit of system parameters we have either homogeneous oscillation or stationary dissipative structures. In a certain way, this is similar to the case that we have for integer derivative indices. Nonlinear dynamics corresponding to these roots is represented by Figs. 7(a)–7(c). For example, at certain parameters we get sufficiently smooth homogeneous oscillations. A decrease of α leads to the interplay between structures that arise from the Hopf and Turing bifurcations [Fig. 7(c)]. A successive decrease of α leads to stable inhomogeneous structures [Fig. 7(b)].

For $\alpha_1 \lesssim \alpha_2$, the diversity of the structure formation increases and we can find the solutions similar to those presented in Figs. 4 and 5. This is due to the fact that the Turing and Hopf bifurcations have independent parameters for their realization. The Turing bifurcation depends on the ratio of the characteristic lengths and is connected with the instability domain $|\bar{n}_1|<1$. The Hopf bifurcation is not connected with the domain $|\bar{n}_1|<1$ and is realized at a wide spectrum of parameters $\alpha_1<\alpha_2$. This makes it possible to find the scenario of a complicated pattern formation due to the interplay between these two types of instabilities. Even in the linear theory, we can find conditions of oscillatory instability for $k\neq 0$ practically not realized at $\alpha_2/\alpha_1=2$. In this case, the inhomogeneous fluctuation becomes unstable according to oscillatory perturbations, and nonlinear structures are similar to those presented in Fig. 2.

V. CONCLUSION

The present study focuses on the influence of the order of fractional derivative indices on pattern formation in fractional reaction-diffusion systems. We showed that in a wide spectrum of parameters, describing the system from a practically elliptic case to hyperbolic systems, we have a diversity of complex pattern formation. In contrast to a standard RDS with integer indices, here the fractional RDS possesses properties connected with the emergence of new types of bifurcations due to fractional derivative indices. We showed that in the case of a small order of derivatives $(\alpha<1)$, the diversity of pattern formation is comparable to the diversity of pattern formation at $\alpha>1$, up to values of $\alpha \simeq 2$ describing practically two-component distributed oscillatory media. Finally, we wish to remark here that spatiotemporal pattern formation phenomena realized in fractional order RDSs have to stimulate experimental investigation of these phenomena in distributive circuits created with the help of modern solid-state electronics [20–22].

[1] G. Nicolis and I. Prigogine, *Self-Organization in Non-Equilibrium Systems* (Wiley, New York, 1977).
[2] M. C. Cross and P. C. Hohenberg, Rev. Mod. Phys. **65**, 851 (1993).
[3] B. S. Kerner and V. V. Osipov, *Autosolitons* (Kluwer, Dordrecht, 1994).
[4] G. M. Zaslavsky, Phys. Rep. **371**, 461 (2002).
[5] R. Metzler and J. Klafter, Phys. Rep. **339**, 1 (2000).
[6] B. I. Henry, T. A. M. Langlands, and S. L. Wearne, Phys. Rev. E **72**, 026101 (2005).
[7] B. I. Henry and S. L. Wearne, Physica A **276**, 448 (2000).
[8] T. A. M. Langlands, B. I. Henry, and S. L. Wearne, Phys. Rev. E **77**, 021111 (2008).
[9] B. I. Henry, T. A. M. Langlands, and S. L. Wearne, Phys. Rev. E **74**, 031116 (2006).
[10] V. Gafiychuk and B. Datsko, Physica A **365**, 300 (2006).
[11] V. Gafiychuk and B. Datsko, Phys. Lett. A **372**, 619 (2008).
[12] V. V. Gafiychuk and B. Y. Datsko, Phys. Rev. E **75**, 055201(R) (2007).
[13] R. Gorenflo and E. A. Abdel-Rehim, J. Comput. Appl. Math. **205**, 881 (2007).
[14] V. Gafiychuk and B. Datsko, Appl. Math. Comput. **198**, 260 (2008).
[15] G. Hornung, B. Berkowitz, and N. Barkai, Phys. Rev. E **72**, 041916 (2005).
[16] A. Iomin, Phys. Rev. E **73**, 061918 (2006).
[17] T. Kosztolowicz, K. Dworecki, and St. Mrowczyński, Phys. Rev. Lett. **94**, 170602 (2005).
[18] J. F. Valdes-Parad, J. A. Ochoa-Tapia, and J. Alvarez-Ramirez, Physica A **369**, 318 (2006).
[19] V. V. Uchaikin and R. T. Sibatov, Commun. Nonlinear Sci. Numer. Simul. **13**, 15 (2008).
[20] A. Adamatzky, B. D. Costello, and T. Asai, *Reaction-Diffusion Computers* (Elsevier, Boston, 2005).
[21] T. Asai, Y. Kanazawa, T. Hirose, and Y. Amemiya, Int. J. Unconv. Comput. **1**, 123 (2005).
[22] T. Serrano-Gotarredona, IEEE Trans. Neural Netw. **14**, 1337 (2003).

[23] I. Petráš, Chaos, Solitons Fractals **38**, 140 (2008).
[24] I. Podlubny *et al.*, Nonlinear Dyn. **29**, 281 (2002).
[25] S. G. Samko, A. A. Kilbas, and O. I. Marichev, *Fractional Integrals and Derivatives: Theory and Applications* (Gordon and Breach, Newark, NJ, 1993).
[26] I. Podlubny, *Fractional Differential Equations* (Academic, New York, 1999).
[27] D. Matignon, *Computational Engineering in System Application* IMACS (IEEE-SMC, Lille, France, 1996), Vol. 2, p. 963.
[28] V. Gafiychuk, B. Datsko, and V. Meleshko, Physica A **387**, 418 (2008).
[29] X. Yuan, T. Teramoto, and Y. Nishiura, Phys. Rev. E **75**, 036220 (2007).
[30] P. Hoffmann, S. Wehner, D. Schmeisser, H. R. Brand, and J. Kuppers, Phys. Rev. E **73**, 056123 (2006).
[31] Y. Hayase and T. Ohta, Phys. Rev. E **66**, 036218 (2002).